Influence of SST Forcing on Stochastic Characteristics of Simulated Precipitation and Drought

IAN M. FERGUSON

Department of Geology and Geological Engineering, Colorado School of Mines, Golden, Colorado

JOHN A. DRACUP

Department of Civil and Environmental Engineering, University of California, Berkeley, Berkeley, California

PHILIP B. DUFFY*

Lawrence Livermore National Laboratory, Livermore, and Climate Central, Inc., Palto Alto, California

PHILIP PEGION+ AND SIEGFRIED SCHUBERT

Global Modeling and Assimilation Office, NASA Goddard Space Flight Center, Greenbelt, Maryland

(Manuscript received 3 December 2008, in final form 17 November 2009)

ABSTRACT

Recent studies demonstrate that ocean–atmosphere forcing by persistent sea surface temperature (SST) anomalies is a primary driver of seasonal-to-interannual hydroclimatic variability, including drought events. Other studies, however, conclude that although SST anomalies influence the timing of drought events, their duration and magnitude over continental regions is largely governed by land–atmosphere feedbacks. Here the authors evaluate the direct influence of SST anomalies on the stochastic characteristics of precipitation and drought in two ensembles of AGCM simulations forced with observed (interannually varying) monthly SST and their climatological annual cycle, respectively. Results demonstrate that ocean–atmosphere forcing contributes to the magnitude and persistence of simulated seasonal precipitation anomalies throughout the tropics but over few mid- and high-latitude regions. Significant autocorrelation of simulated seasonal anomalies over oceans is directly forced by persistent SST anomalies; over land, SST anomalies are shown to enhance autocorrelation associated with land–atmosphere feedbacks. SST anomalies are shown to have no significant influence on simulated drought frequency, duration, or magnitude over most midlatitude land regions. Results suggest that severe and sustained drought events may occur in the absence of persistent SST forcing and support recent conclusions that ocean–atmosphere forcing primarily influences the timing of drought events, while duration and magnitude are governed by other mechanisms such as land–atmosphere feedbacks. Further analysis is needed to assess the potential model dependence of results and to quantify the relative contribution of land–atmosphere feedbacks to the long-term stochastic characteristics of precipitation and drought.

1. Introduction

Drought affects virtually all human and environmental systems. Despite tremendous investments in water resources planning and management, drought remains the costliest of natural disasters—in the United States alone, drought causes an average of \$6–\$8 billion (U.S. dollars) per year in direct and indirect economic effects (e.g., Wilhite and Buchanan-Smith 2005). Many regions

* Current affiliation: Climate Central, Inc., Palo Alto, California.
+ Current affiliation: NOAA/Earth System Research Laboratory/Physical Sciences Division, Boulder, Colorado.

Corresponding author address: Ian M. Ferguson, Geology and Geological Engineering, Colorado School of Mines, Golden, CO 80403.
E-mail: imfergus@mines.edu

DOI: 10.1175/2009JHM1132.1

© 2010 American Meteorological Society

in the United States and abroad are becoming increasingly vulnerable to drought as a result of population and industrial growth, hardening water demands, and contamination of surface and groundwater supplies (California DWR 2000). Moreover, anthropogenic climate change is altering the hydrologic cycle at global and regional scales (e.g., Barnett et al. 2008); recent studies suggest that climate change is likely to result in drier conditions over continental interiors during summer as well as increased occurrence of extreme drought events (Bates et al. 2008). However, the potential effects of climate change on the stochastic characteristics of precipitation and drought—including probability distributions of drought duration and magnitude—cannot be confidently assessed without better understanding the fundamental mechanisms of drought.

The immediate cause of drought is below-normal precipitation over a given region for a sustained period of time (e.g., Keyantash and Dracup 2002; Wilhite and Buchanan-Smith 2005). However, it is widely accepted that the short time scales and chaotic nature of the atmosphere generally limit the persistence of internal atmospheric perturbations—including precipitation-bearing weather systems—to subseasonal time scales (e.g., Lorenz 1963; Palmer 2000). It has therefore been hypothesized that persistent atmospheric and hydroclimatic anomalies—including drought events—are driven primarily by mechanisms external to the atmosphere (e.g., Van den Dool and Chervin 1986; Palmer 2000; Hoerling and Kumar 2003; Schubert et al. 2004a,b).

Numerous studies have demonstrated significant relationships between sea surface temperature (SST) and hydroclimatic variability. For example, observed precipitation and streamflow anomalies over many regions around the world are significantly correlated with the El Niño–Southern Oscillation (ENSO; Ropeleski and Halpert 1987; Redmond and Koch 1991; Dracup and Kahya 1994; and many others). With respect to drought, Seager (2007) showed that six historical periods of widespread drought conditions across North America—including the 1930s ''Dust Bowl'' drought, which affected more than 60% of the United States—each coincided with persistent ''La Nina like'' SST anomalies in the tropical Pacific (i.e., warm SST anomalies in the western tropical Pacific and cool SST anomalies in the eastern tropical Pacific). Other studies suggest that decadal-scale variability in extratropical SST contribute to decadal variability in drought frequency and magnitude (McCabe et al. 2004; Hidalgo 2004).

A number of modeling studies have further demonstrated the strong influence of SST anomalies on both the timing and magnitude of precipitation anomalies over much of the globe (Koster et al. 2000; Shukla et al. 2000; Zwiers et al. 2000; Straus et al. 2003). In the context of drought, Hoerling and Kumar (2003) used an ensemble of atmospheric general circulation model (AGCM) experiments to show that widespread midlatitude drought conditions during 1998–2002 were largely driven by persistent La Niña conditions in conjunction with warm SST anomalies in the Indian Ocean. Similarly, Schubert et al. (2004b) and Seager et al. (2005) showed that ensembles of AGCM simulations forced with observed twentieth-century SST reproduced much of the observed low-frequency variability in twentieth-century precipitation over the U.S. Great Plains, including the timing and duration of major droughts of the 1930s and 1950s. These studies suggest that ocean–atmosphere forcing by persistent SST anomalies is a primary driver of seasonal-to-interannual hydroclimatic variability over much of the globe, including severe and sustained drought events.

In addition to ocean–atmosphere forcing, recent studies have shown that land–atmosphere feedbacks also contribute to the magnitude and persistence of precipitation anomalies and drought events over continental regions. Findell and Eltahir (1997) and Eltahir (1998) demonstrated significant positive correlation between observed soil moisture and subsequent precipitation over the U.S. Great Plains during summer. Koster et al. (2003) compared the mean, variance, and autocorrelation of observed precipitation to those of precipitation from AGCM simulations carried out with and without land–atmosphere feedbacks. Their results suggest that land–atmosphere feedbacks play an important role in governing the magnitude and persistence of precipitation anomalies over land. Similar modeling studies suggest that land–atmosphere feedbacks contribute to the magnitude and persistence of extreme events such as droughts and heat waves (Hong and Kalnay 2000; Schubert et al. 2004a; Fischer et al. 2007; Pegion and Kumar 2008).

Despite numerous studies on the relative contributions of ocean–atmosphere forcing and land–atmosphere feedbacks to the duration and magnitude of individual drought events, the influence of ocean–atmosphere forcing on the long-term stochastic characteristics of precipitation anomalies and drought—as opposed to individual drought events—has not been evaluated. In this study, we evaluate the influence of ocean–atmosphere forcing on stochastic characteristics of precipitation and drought that are commonly used in water resources planning and management, including seasonal mean precipitation, the magnitude and persistence of precipitation anomalies, and the frequency, duration, and magnitude of drought events at seasonal-to-multiyear time scales.

The relatively short historical record and sparse observational coverage over much of the globe largely

precludes observational drought analysis. In addition, the inherent coupling of ocean, land, and atmosphere processes complicates observation-based analyses of the physical mechanisms of drought. By contrast, AGCMs allow us to extend the data record by carrying out multiple realizations and provide spatially and temporally complete records of (simulated) climate variables. AGCMs also allow us to isolate the influence of SST forcing through numerical experiments with idealized SST boundary conditions. We therefore evaluate the effect of SST anomalies on seasonal precipitation and drought characteristics by comparing two ensembles of AGCM simulations forced with observed (interannually varying) monthly SST and their climatological annual cycle, respectively.

2. Model and data

We analyze precipitation and drought characteristics in two ensembles of simulations with version 1 of the National Aeronautics and Space Administration (NASA) Seasonal-to-Interannual Prediction Project (NSIPP) AGCM, NSIPP-1. NSIPP-1 is a gridpoint model with a finite difference dynamical core (Suarez and Takacs 1995). A simple K scheme calculates turbulent diffusivities for heat and momentum in the boundary layer based on Monin–Obukov similarity theory, and convection is parameterized using the relaxed Arakawa–Schubert scheme (Arakawa and Schubert 1974; Moorthi and Suarez 1992). Land surface processes are represented by the Mosaic land surface model, with vegetation parameters described by a climatological cycle as detailed in Koster and Suarez (1996). Details of NSIPP-1 model formulation and its climate are described in Bacmeister et al. (2000).

NSIPP-1 was developed with particular emphasis on accurate simulation of tropical ocean–atmosphere interaction, midlatitude stationary waves, and extratropical response to tropical SST anomalies. While NSIPP-1 does exhibit biases in the magnitude of seasonal means and variances over some regions, pattern correlations between seasonal mean precipitation fields from the Global Precipitation Climatology Project (GPCP) observational dataset[1] (Adler et al. 2003) and NSIPP-1 simulations are 0.84 for December–February (DJF) and 0.79 for June–August (JJA); spatial correlations between observed and simulated variance fields are 0.82 for DJF and 0.73 for JJA. All pattern correlations are statistically significant (by normal approximation to Fisher's z transform, subsampled to account for spatial autocorrelation; $\alpha = 0.05$). Autocorrelation of simulated seasonal precipitation anomalies is significantly different from observed over less than 5% of the globe and less than 7% of global land areas, and the differences are not field significant (as per Livezey and Chen 1983; $\alpha = 0.05$). Lastly, observed and simulated correlations between seasonal precipitation anomalies and seasonal SST anomalies over the Niño-3.4 region of the tropical Pacific—a common ENSO index—are significantly different over less than 15% of the globe for both DJF and JJA, and differences are not field significant (as per Livezey and Chen 1983; $\alpha = 0.05$). NSIPP-1 thus reproduces quite well the salient features of observed seasonal precipitation and ENSO teleconnections when forced with observed SST.

The two ensembles evaluated here were carried out at the NASA Goddard Space Flight Center as part of the Climate of the 20th Century project (Folland et al. 2002). The first ensemble consists of 14 simulations of the twentieth century (1902–2001) forced with prescribed observed monthly-mean SST (hereafter referred to as observed SST simulations); the second consists of four 50-yr simulations with the same model but forced with the climatological annual cycle of twentieth-century SST (hereafter referred to as climatological SST simulations). Because droughts are by definition rare events, all relevant and available simulations were used to maximize the degrees of freedom in hypothesis tests of differences in drought characteristics between ensembles. It should be noted that all hypothesis tests used in this study explicitly account for differences in ensemble size; results of hypothesis tests between the climatological SST ensemble and an equal size subset of the observed SST ensemble are qualitatively identical to those presented later, though the extent of statistical significance is reduced because of the reduction in degrees of freedom.

All simulations were carried out with identical atmospheric composition and solar insolation. Within each ensemble, simulations were forced with identical SST boundary conditions; ensemble members differ only in their atmospheric initial conditions, which were slightly perturbed in each case. Prescribed SST boundary conditions were derived from the Met Office Hadley Centre Sea Ice and Sea Surface Temperature dataset version 1 (HadISST1) global SST and sea ice dataset (Rayner et al. 2003), and land surface boundary conditions were determined interactively by the Mosaic land surface model. For computational feasibility, simulations were run at a relatively coarse resolution of 3.0° latitude × 3.75° longitude with 34 unevenly distributed vertical levels. The observed SST simulations used here were previous analyzed by Schubert et al. (2004b, 2008), and were found to capture much of the low-frequency variability in precipitation over the U.S. Great Plains, including the Dust Bowl drought of the 1930s and the severe drought of the 1950s.

[1] All comparisons to the GPCP observational dataset were carried out for the period 1980–2001.

Seasonal precipitation was calculated by aggregating daily precipitation in each simulation over each of four seasons: DJF, March–May (MAM), JJA, and September–November (SON). Seasonal anomalies were subsequently calculated by removing the respective seasonal means, taken as the average over all observed SST simulations for the 1961–90 base period.

Drought conditions were defined at the n = 3-, 12-, 24-, and 48-month time scales using the standardized precipitation index (SPI; McKee et al. 1993; Guttman 1999). SPI is essentially a statistical transformation of the probability density function of the n-month total precipitation at a given location and time of year to a standard normal (Gaussian) distribution. SPI thus has a clearly defined physical basis in terms of cumulative moisture availability, as well as a sound statistical basis in terms of the standard normal distribution. For each time scale n, month k ($k = 1, 2, \ldots, 12$), and model grid cell, a gamma distribution was fit to the distribution of total precipitation for the 1961–90 base period, pooled over all observed SST ensemble members. Precipitation values were converted to cumulative density values based on the fitted gamma distributions; SPI values were subsequently calculated by transforming cumulative densities to standard normal Z values (Guttman 1999; Hayes et al. 1999; Lloyd-Hughes and Saunders 2002). The median value of total precipitation over a given period thus corresponds to a SPI value of zero, with the 10th and 90th percentiles of total precipitation corresponding to SPI values of -1.645 and 1.645, respectively.

A threshold of SPI ≤ -1.0 is commonly used to define moderate drought conditions and is used here to define drought events in each simulation (Hayes et al. 1999; NOAA 2009; WRCC 2009). For each time scale, discrete drought events were identified as beginning when SPI falls below -1.0 and ending when SPI returns to zero (e.g., Maidment 1993; McKee et al. 1993; Keyantash and Dracup 2002; Sheffield et al. 2004; Andreadis et al. 2005; Quiring and Goodrich 2008). For each event, drought duration was defined as the number of consecutive months between drought onset and termination and drought magnitude was defined as the average monthly precipitation deficit over this duration (i.e., the mean monthly precipitation anomaly during a drought event). It should be noted that spatial aspects of drought are not considered in this analysis.

Time series of simulated SPI over the U.S. Great Plains region from the first observed SST simulation are shown in Fig. 1 to illustrate the time scales of variability considered. While SPI is clearly a meteorological index, the flexibility of SPI with respect to time scale makes it amenable to monitoring multiple aspects of drought. Root zone soil moisture anomalies and agricultural drought indices, for example, are strongly correlated with SPI at time scales of 1–3 months, while streamflow is strongly correlated with SPI at time scales of 9–12 months (e.g., McKee et al. 1993; Seiler et al. 2002; Sims et al. 2002; Nalbantis and Tsakiris 2009). SPI at 1–3 month time scales is also correlated with vegetation productivity as measured by the normalized difference vegetation index (NDVI; Ji and Peters 2003). At 24- and 48-month time scales, SPI is correlated with variations in groundwater levels and is representative of accumulated multiyear moisture deficits associated with persistent droughts and low-frequency hydroclimatic variability (McKee et al. 1993; Mishra and Desai 2005). SPI is thus gaining popularity among the drought monitoring and research communities due to its flexibility, transparency, and sound physical and statistical bases (Keyantash and Dracup 2002; M. Svoboda 2008, personal communication; K. T. Redmond 2006, personal communication).

3. Comparison of seasonal precipitation characteristics

Precipitation is a significant driver of the terrestrial hydrologic cycle—including soil moisture, surface water, and groundwater availability—and interannual precipitation variability affects a broad range of human and natural systems. Water resources planning and management are founded on the stochastic characterization of regional precipitation and drought, and three precipitation characteristics are of critical importance: seasonal mean precipitation, its interannual variance, and the persistence of seasonal anomalies. While a number of studies have evaluated correlations between precipitation anomalies and SST and the influence of SST on interannual variability of precipitation, the influence of SST anomalies on long-term mean precipitation and persistence of precipitation anomalies has not been evaluated. In this section, we assess the effect of SST anomalies on the stochastic characteristics of seasonal precipitation by comparing the observed and climatological SST ensembles; the effect of SST anomalies on stochastic characteristics of drought is evaluated in section 4.

a. Seasonal mean precipitation

To evaluate the influence of SST anomalies on seasonal mean precipitation, we conduct a two-tailed Mann–Whitney (MW) test. Because seasonal precipitation is not normally distributed over much of the globe, the standard t test is not strictly valid (von Storch and Zwiers 1999; Zar 1999); the MW test is a nonparametric test of the difference between the center (mean) of sample distributions and is applicable in cases where the standard t test is not valid. We apply the MW test at each

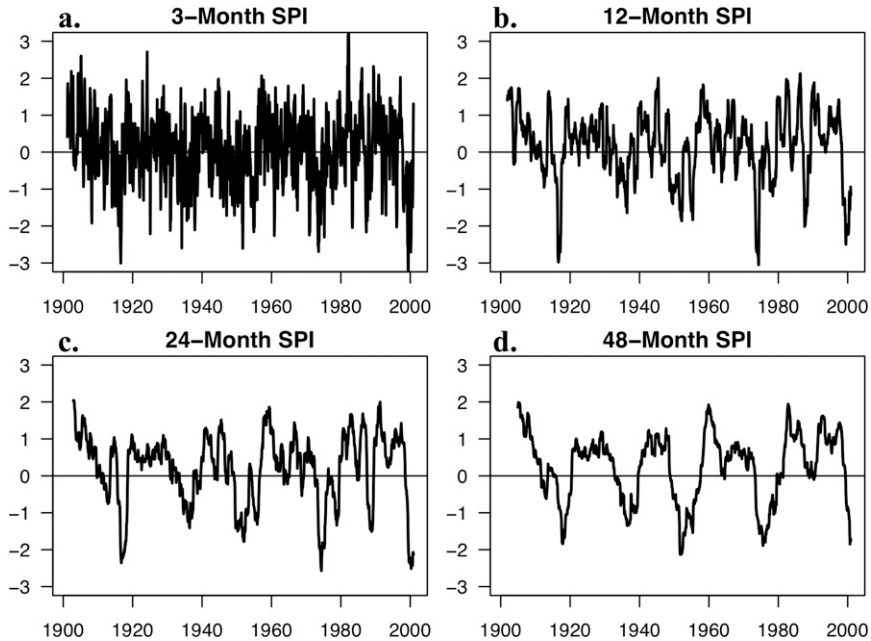

FIG. 1. Time series of SPI over the U.S. Great Plains from simulation 1 of the observed SST ensemble for the (a) 3-, (b) 12-, (c) 24-, and (d) 48-month time scales.

model grid cell with the two-tailed null hypothesis H_o: $\overline{x}_{\text{Observed-SST},k} = \overline{x}_{\text{Climatological-SST},k}$, where $\overline{x}_{\text{Observed-SST},k}$ and $\overline{x}_{\text{Climatological-SST},k}$ are seasonal mean precipitation for season k averaged over all observed and climatological SST simulations, respectively.

Figure 2 shows the difference in seasonal mean precipitation (mm) between observed and climatological SST ensembles, masked (gray) where differences are not statistically significant at the $\alpha = 0.05$ level. Significant differences occur over 23.5% (24.6%) of the cosine-weighted global area (global land area) for DJF, 23.7% (24.9%) for MAM, 20.0% (21.4%) for JJA, and 22.6% (22.7%) for SON. Significant differences are located predominately over tropical–subtropical boundaries, suggesting that interannual variability of SST affects long-term mean circulation patterns, including patterns of tropical convection, subtropical subsidence, and midlatitude moisture convergence. With the exception of DJF, the largest regions of significant difference occur over the tropical–subtropical transition regions, where absolute differences exceed 50 mm per season, as much as a 50% change in seasonal precipitation.

Differences are generally not consistent across seasons. For DJF and JJA, approximately half of the significant differences are positive ($\overline{x}_{\text{Observed-SST},k} > \overline{x}_{\text{Climatological-SST},k}$) and half are negative. For MAM, precipitation is greater in the observed than climatological SST simulations for 75.3% of the total area of significant differences, while for SON it is greater over only 18.5%. Because tropical convection influences moisture transport and precipitation over much of the globe, asymmetry in the influence of SST anomalies on mean precipitation between MAM and SON is likely due to SSTs being warmest during MAM and coolest during SON and the dependence of tropical moist convection on absolute SST (rather than SST anomalies) via the Causius–Clapeyron relation (e.g., Graham and Barnett 1987).

Significant differences in seasonal mean precipitation between observed and climatological SST ensembles is indicative of asymmetry in the precipitation response to SST forcing over some regions—that is, the precipitation response to positive SST anomalies is not equal and opposite to its response to negative SST anomalies. Results imply that changes in SST variability—in addition to mean SST—will affect long-term seasonal mean precipitation over these regions. However, the lack of significant differences over most regions supports previous results that suggest the precipitation response to SST anomalies is predominately linear over much of the globe (e.g., Quan et al. 2006).

b. *Interannual variance*

By definition, seasonal precipitation anomalies—and ultimately droughts—result from interannual variability of seasonal precipitation about its climatological mean. Previous modeling studies have shown greater interannual precipitation variability in simulations carried out with

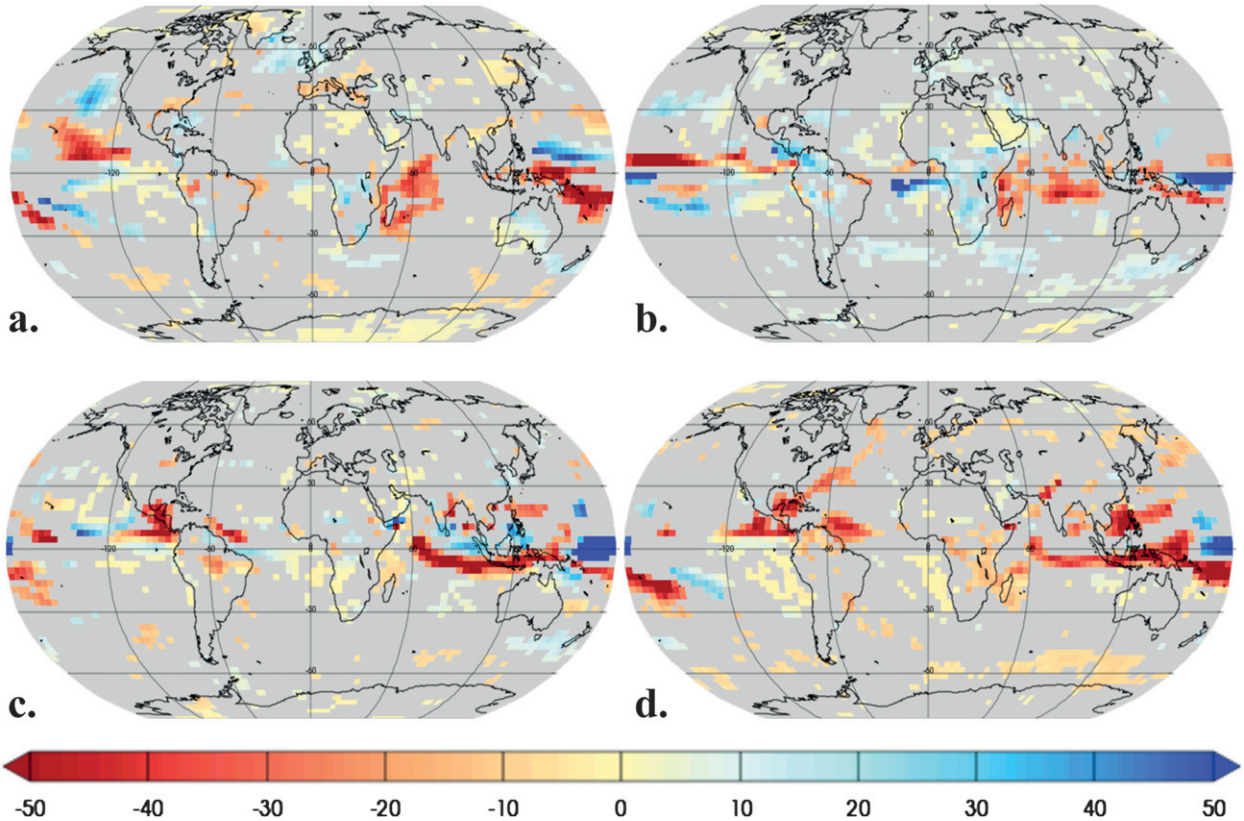

FIG. 2. Differences in seasonal mean precipitation (mm) between observed and climatological SST simulations for (a) DJF, (b) MAM, (c) JJA, and (d) SON. Values are masked (gray) where differences are not statistically significant according to the MW test ($\alpha = 0.05$).

observed (interannually varying) SST boundary conditions compared to simulations carried out with climatological SST (e.g., Koster et al. 2000). Here we compare the magnitude of precipitation anomalies between observed and climatological SST ensembles as a precursor to evaluating the influence of SST anomalies on drought magnitudes (see next section).

Like the t test, the standard variance ratio test is sensitive to nonnormality; we therefore compare interannual variability of seasonal precipitation between observed and climatological SST ensembles using a nonparametric rank sum (RS) test of dispersion. The RS test is equivalent to applying the MW test to the *absolute deviations* of seasonal precipitation (von Storch and Zwiers 1999). Because we expect SST forcing to increase interannual variability (e.g., Koster et al. 2000), we test the one-sided null hypothesis H_o: $\sigma^2_{\text{Observed-SST},k} \leq \sigma^2_{\text{Climatological-SST},k}$, where $\sigma^2_{\text{Observed-SST},k}$ and $\sigma^2_{\text{Climatological-SST},k}$ are variances of seasonal precipitation in the observed and climatological SST ensembles for season k, respectively.

Figure 3 shows the ratio of $\sigma^2_{\text{Observed-SST},k}$ to $\sigma^2_{\text{Climatological-SST},k}$ for each season, masked where $\sigma^2_{\text{Observed-SST},k}$ is not significantly greater than $\sigma^2_{\text{Climatological-SST},k}$ ($\alpha = 0.05$). Significant differences are widespread and spatially coherent, with 49.2% (43.1%) of the globe (global land) exhibiting a significant difference for DJF, 55.3% (50.3%) for MAM, 55.5% (47.3%) for JJA, and 46.3% (47.3%) for SON. Over the tropical Pacific, interannual variability in the observed SST ensemble is more than 5 times that in the climatological SST ensemble, and variability in the observed SST ensemble is more than 2 times that in the climatological SST ensemble throughout much of the tropics during all seasons. Variability in the observed SST ensemble is between 25% and 50% greater than in the climatological SST ensemble over several midlatitude land regions, particularly in the Southern Hemisphere. Results are similar to those in previous studies (e.g., Koster et al. 2000).

c. *Persistence of seasonal anomalies*

The persistence of precipitation anomalies from one season to the next is fundamental to the occurrence of sustained droughts and wet spells, and autocorrelation analysis is an important component of water resources planning and management. While a number of recent studies suggest that SST anomalies are a primary driver of seasonal-to-interannual hydroclimatic variability over

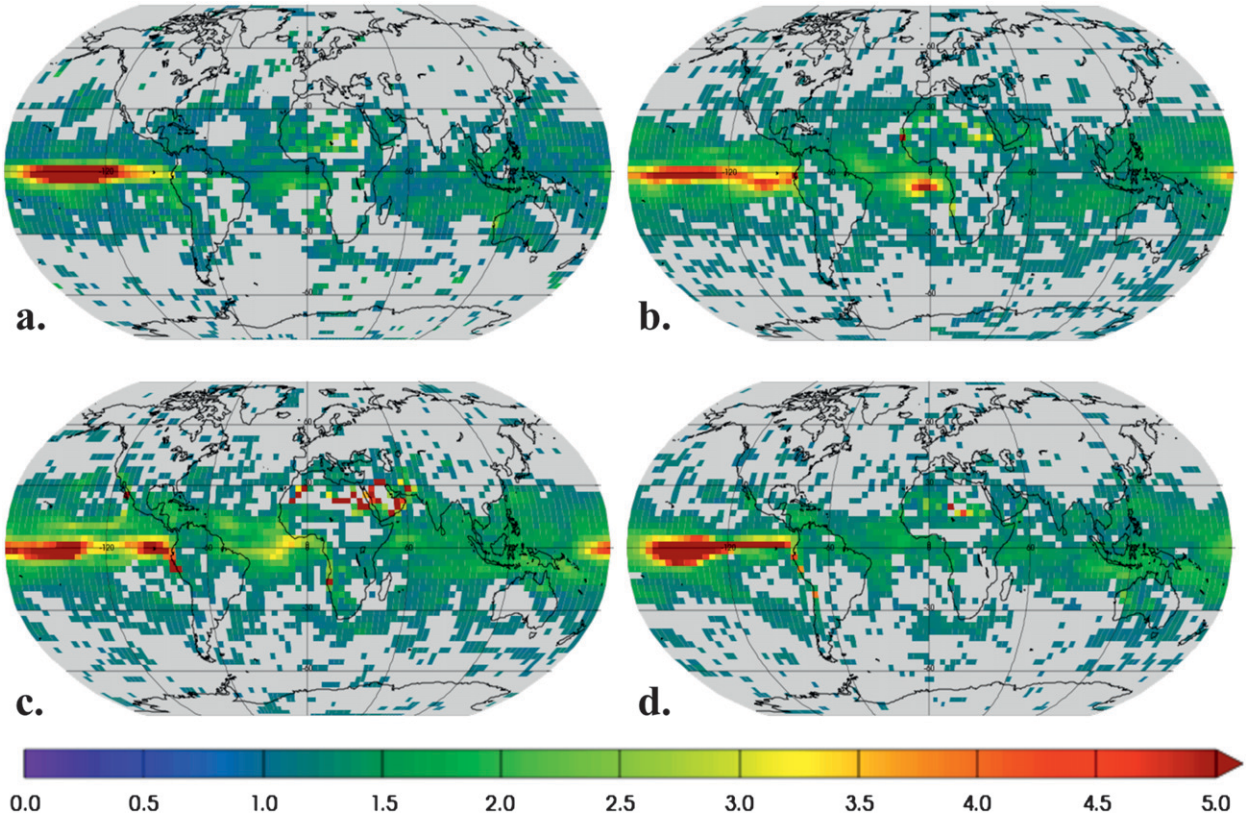

FIG. 3. Variance ratio between observed and climatological SST simulations ($\sigma^2_{\text{Observed-SST}}/\sigma^2_{\text{Climatological-SST}}$) for (a) DJF, (b) MAM, (c) JJA, and (d) SON, masked (gray) where $\sigma^2_{\text{Observed-SST}}$ is not significantly $>\sigma^2_{\text{Climatological-SST}}$ based on the RS test of dispersion ($\alpha = 0.05$).

much of the globe, the influence of SST anomalies on the persistence of precipitation anomalies has not been directly evaluated. Here we compare the lag-1 autocorrelation of seasonal precipitation anomalies averaged over the observed and climatological SST ensembles. Seasonal anomalies are calculated as detailed in section 2; autocorrelations are calculated aggregated over all four seasons as per von Storch and Zwiers (1999). Using the normal approximation to Fisher's z-transform test (e.g., Zar 1999), we evaluate the statistical significance of lag-1 autocorrelations from each ensemble—that is, we test the one-sample null hypothesis H_o: $r_1 \leq 0.0$, where r_1 is the lag-1 autocorrelation of seasonal anomalies over a given ensemble. We then compare lag-1 autocorrelations in the observed and climatological SST ensembles; because we expect SST forcing to increase persistence, we test the one-sided null hypothesis H_o: $r_{1,\text{Observed-SST}} \leq r_{1,\text{Climatological-SST}}$.

Figures 4a and 4b show the global distributions of $r_{1,\text{Observed-SST}}$ and $r_{1,\text{Climatological-SST}}$, respectively, masked where values are not significantly greater than zero ($\alpha = 0.05$). For comparison, Fig. 4c shows the lag-1 autocorrelation of seasonal SST anomalies in the HadISST forcing dataset. Seasonal autocorrelation in the observed SST simulation exceeds 0.65 over the tropical Pacific and exceeds 0.3 throughout much of the tropics; autocorrelation decreases rapidly with latitude, with values generally ranging from 0.0 to 0.2 over mid- and high latitudes. By contrast, autocorrelation in the climatological SST simulation does not exceed 0.25 over any region. In the observed SST ensemble, seasonal autocorrelation is significantly greater than zero over 50.7% of the globe (44.7% of global land), including most of the tropics and large midlatitude land and ocean regions. In the climatological SST ensemble, seasonal autocorrelation is significant over only 2.7% of the globe (5.1% of global land). Significant autocorrelation in the climatological SST ensemble largely coincides with "hot spots" of land–atmosphere coupling identified in previous studies (Koster et al. 2003, 2004), suggesting that autocorrelation in this ensemble is largely driven by land–atmosphere feedbacks.

Analysis of autocorrelation by season (i.e., persistence from winter to spring and summer to fall, respectively) shows similar results to those in Figs. 4a and 4b over oceans but clear differences over land. Most notably, significant autocorrelation over central North America and South America occurs only from summer to fall in

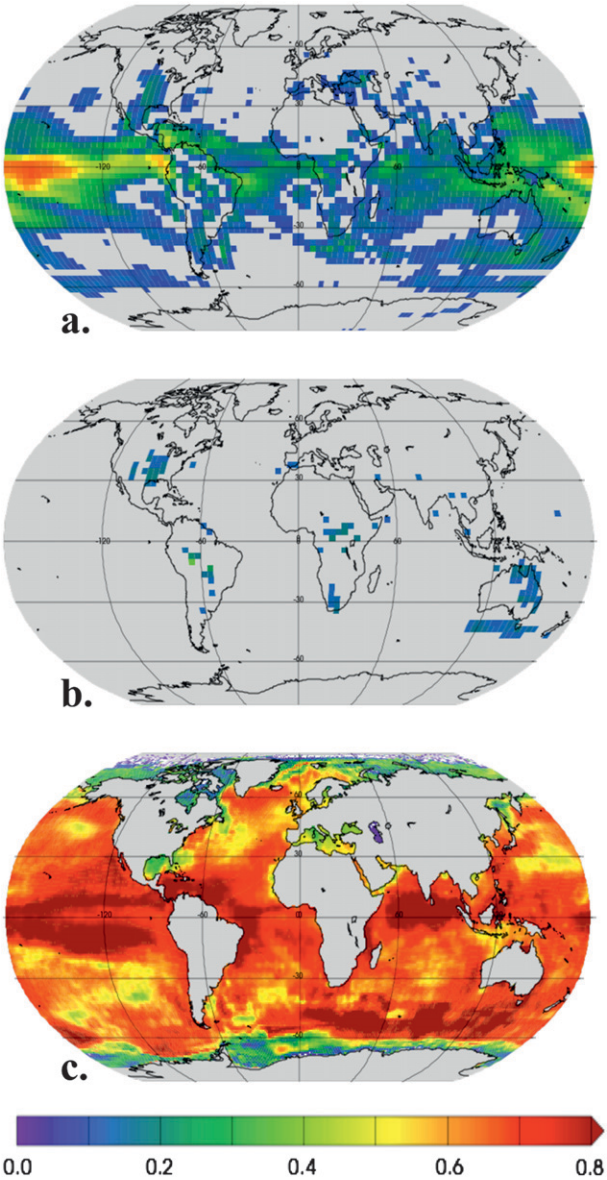

FIG. 4. Lag-1 autocorrelation of seasonal precipitation anomalies from (a) observed ($r_{1,\text{Observed-SST}}$) and (b) climatological ($r_{1,\text{Climatological-SST}}$) SST ensembles, averaged across all ensemble members. (c) Lag-1 autocorrelation of seasonal SST anomalies from HadISST forcing dataset. Values are masked (gray) where not significantly >0 (Fisher's z transform, $\alpha = 0.05$).

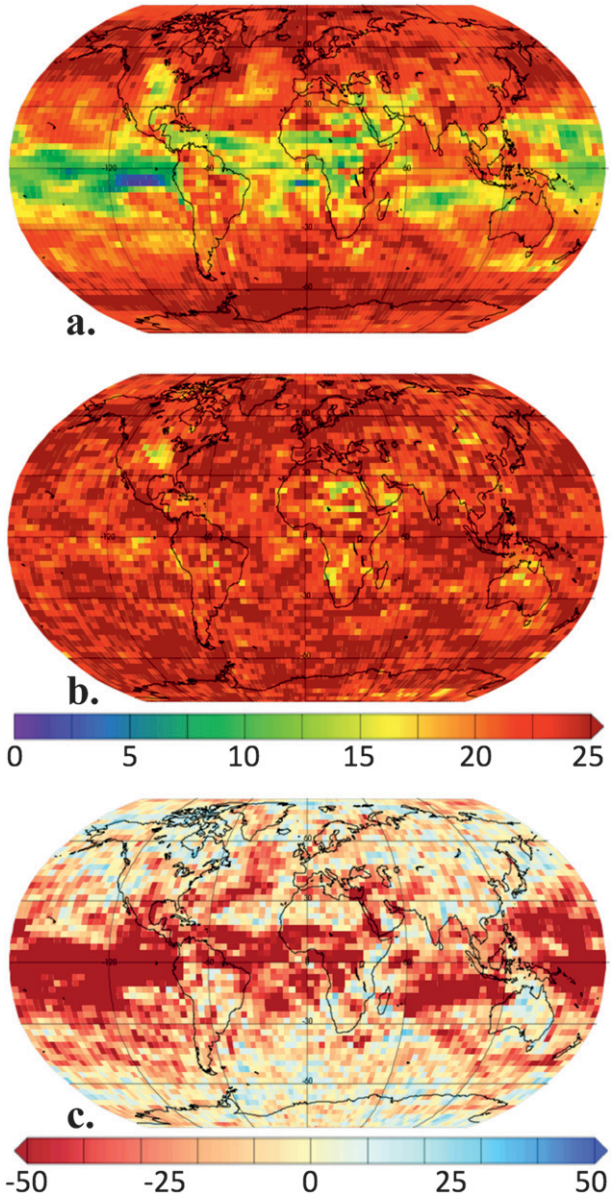

FIG. 5. Mean drought frequency (drought events per century) of drought events defined using the 12-month SPI from (a) observed and (b) climatological SST ensembles, and (c) the percent difference between the two (observed SST – climatological SST).

both ensembles, while significant autocorrelation over southern Africa and Australia occurs only from winter to spring. Results are consistent with the influence of land–atmosphere feedbacks, which are strongest during summer when the land surface is predominately moisture limited and soil moisture thus has the greatest influence on the surface energy balance. However, the magnitude of autocorrelation and spatial extent of statistical significance over land remains greater in the observed SST ensemble compared to the climatological SST ensemble during both seasons, suggesting that SST anomalies also contribute to the persistence of precipitation anomalies over some midlatitude land regions.

Comparing autocorrelations between the observed and climatological SST ensembles, $r_{1,\text{Observed-SST}}$ is significantly greater than $r_{1,\text{Climatological-SST}}$ over 42.8% of the globe. As expected, significant differences generally occur over regions that exhibit significant autocorrelation in the observed SST ensemble but not in the climatological

SST ensemble. Autocorrelation in the observed SST ensemble is greater than that in the climatological SST ensemble over most land regions, though differences are generally not statistically significant over midlatitudes.

Figure 4 supports the hypothesis that persistent SST anomalies are the dominant driver of seasonal persistence of atmospheric anomalies over much of the globe. While significant persistence over several midlatitude land regions in the climatological SST ensemble supports the previous conclusion that land–atmosphere feedbacks contribute to persistence over these regions, the large increase in magnitude and spatial extent of significant autocorrelation over these regions in the observed SST ensemble suggests that ocean–atmosphere forcing also contributes to seasonal persistence over land. However, the lack of significant persistence over most mid- and high-latitude regions in both the observed SST and climatological ensembles is indicative of the short time scales and chaotic nature of atmospheric variability over these regions. While SST anomalies can persist from seasons to years, simulated precipitation anomalies over most mid- and high-latitude regions are statistically independent from one season to the next. Serial independence implies that persistent, multiseason periods of below (or above) normal precipitation occur primarily by chance over these regions.

4. Comparison of drought characteristics

Previous studies have shown significant correlation between SST anomalies and drought occurrence over several regions around the globe, and recent case studies suggest that SST anomalies played a major role in several severe historical droughts, including the severe droughts of the 1930s, 1950s, and 1990s over the U.S. Great Plains. However, the influence of SST anomalies on the long-term stochastic characteristics of drought—including empirical distributions of drought frequency, duration, and magnitude—has not been evaluated.

a. Drought frequency

Figure 5 shows the frequency of drought events in the observed and climatological SST ensembles for drought events based on the 12-month SPI (see section 2), along with the percent difference between the two ensembles. Drought frequencies were calculated as the average number of drought events per 100 years in each ensemble. By definition, the probability of drought during any given month based on SPI (i.e., probability of SPI ≤ -1.0) is 0.159. Spatial variability in drought frequency within each ensemble is therefore related to regional differences in the persistence of drought events (i.e., greater frequency is associated with shorter droughts), while differences in drought frequency between ensembles result from the SST-forced changes in precipitation characteristics.

The global pattern of drought frequency in both ensembles clearly corresponds to the global pattern of autocorrelation (Figs. 4a and 4b). In the observed SST ensemble, high autocorrelations of precipitation anomalies throughout the tropics and central North America result in an increase in drought durations and a corresponding decrease in drought frequencies over these regions; in the Climatological ensemble, drought frequencies are uniformly high over most of the globe with the exceptions of central North America, portions of Africa and the Middle East, and northern Australia, corresponding to regions of significant autocorrelation of seasonal precipitation anomalies. Correspondence between global distributions of autocorrelation and drought frequencies defined at the 12-month time scale highlight the strong relationship between seasonal precipitation characteristics and drought characteristics on annual and interannual time scales.

Drought frequencies in the observed SST ensemble are generally less than in the climatological SST ensemble, though several regions of higher drought frequency in the observed SST ensemble occur over mid- and high latitudes. Differences in drought frequency exceed 50% throughout much of the tropics, where SST anomalies have the strongest influence on persistence of precipitation anomalies. Over mid- and high-latitudes, differences are less than 15% over most land regions with the exception of parts of central North America, central South America, and the Middle East. Over these regions, higher persistence of seasonal precipitation anomalies contributes to an increase in drought duration and consequently a decrease in drought frequency; however, as shown later, differences in drought duration are not statistically significant over these regions. The small difference in drought frequency over mid- and high latitudes suggests that drought events occur as often ''by chance''—that is, without SST forcing—as under SST-forced conditions. Results are similar for droughts defined at the 3-, 24-, and 48-month time scales (not shown).

b. Drought duration

Empirical distributions of drought duration were compared between ensembles using the MW test, RS test of dispersion, and Kolmogorov–Smirnov (KS) test. As discussed earlier, the MW and RS tests are nonparametric tests for differences between the centers (i.e., means) and dispersions (i.e., variances) of sample distributions, respectively. On the basis of results presented earlier, we expect that SST anomalies will drive an increase in both the mean and dispersion of simulated

drought durations; we therefore test the one-sided null hypotheses H_o: $\overline{D}_{\text{Observed-SST}} \leq \overline{D}_{\text{Climatological}}$ and H_o: $\sigma^2_{D,\text{Observed-SST}} \leq \sigma^2_{D,\text{Climatological}}$, where $\overline{D}_{\text{Observed-SST}}$ and $\overline{D}_{\text{Climatological}}$ are the mean drought durations for the observed and climatological SST ensembles, respectively, and $\sigma^2_{D,\text{Observed-SST}}$ and $\sigma^2_{D,\text{Climatological}}$ are the variances about their respective means.

The KS test is a widely used goodness-of-fit test, but it may also be applied to compare empirical distributions between samples (e.g., von Storch and Zwiers 1999; Zar 1999). The KS test is based on the maximum absolute difference between cumulative frequencies; while relatively weak, its sensitivity to differences in both the center and the tails of the distributions make it a worthwhile, albeit conservative, complement to the MW and RS tests. The KS test assumes the general null hypothesis that the distribution of drought durations in the observed SST ensemble is equal to that in the climatological SST ensemble.

Figure 6a shows the difference in mean drought duration for droughts defined using the 12-month SPI; values are masked (gray) where $\overline{D}_{\text{Observed-SST}}$ is not significantly greater than $\overline{D}_{\text{Climatological-SST}}$ (MW test; $\alpha = 0.05$). As expected, $\overline{D}_{\text{Observed-SST}}$ is significantly greater than $\overline{D}_{\text{Climatological-SST}}$ throughout much of the tropics, with differences exceeding 25 months over some tropical ocean regions. Here $\overline{D}_{\text{Observed-SST}}$ is also significantly greater over several land regions, most notably India, eastern Australia, central South America, and the Pacific Northwest region of North America. Mean drought duration is significantly greater in the observed SST ensemble over 41.9% of the globe, including 32.8% of global land areas. Results are similar for droughts defined at other time scales, with the fraction of global area exhibiting significant differences generally decreasing with increasing time scale (45.4%, 34.0%, and 28.3% at the 3, 24, and 48-month time scales, respectively; not shown).

Figure 6b shows the variance ratio of drought durations between ensembles, again, for drought events defined at the 12-month time scale; values are masked where $\overline{D}_{\text{Observed-SST}}$ is not significantly greater than $\sigma^2_{D,\text{Climatological-SST}}$ (RS test; $\alpha = 0.05$). Similar to mean durations, significant differences encompass 47.5% of the globe, including 40.2% of global land areas. Variability in drought duration in the observed SST ensemble is more than 5 times that of the climatological SST ensemble over many tropical ocean regions and more than 2 times that of the climatological SST ensemble over several land regions. Significant differences are much more widespread at the 3-month time scale, with 89.0% of the globe exhibiting significantly greater variability in drought durations in the observed SST ensemble;

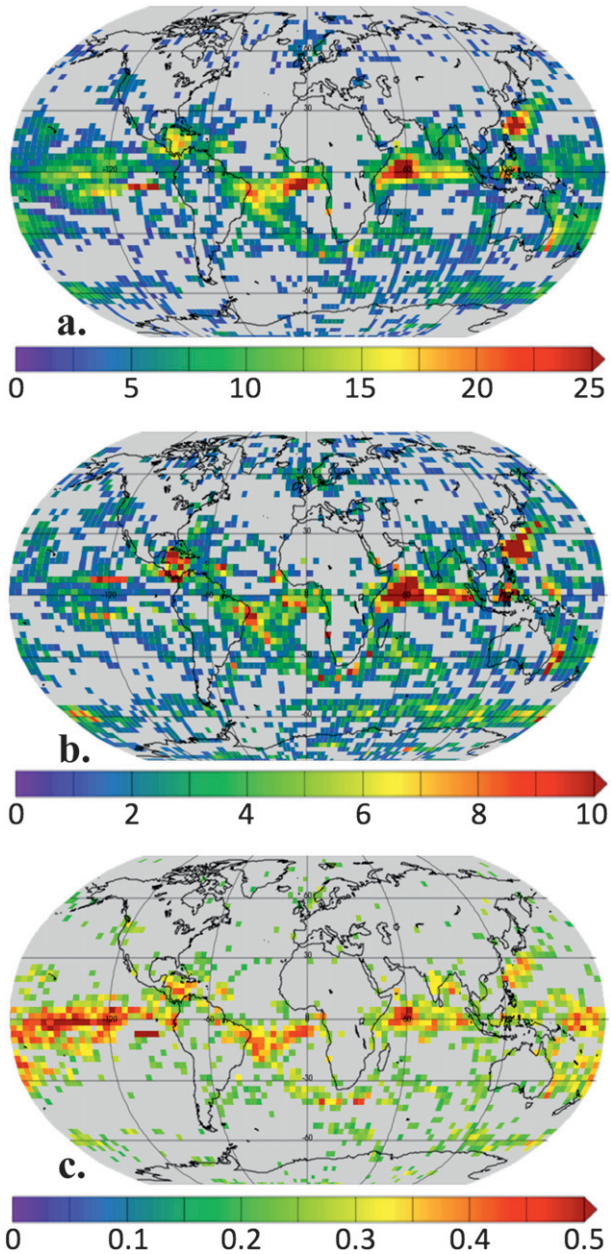

FIG. 6. Hypothesis tests between empirical distributions of drought duration from observed SST and climatological SST ensembles for drought events defined using 12-month SPI. (a) Difference in mean drought duration (months), masked (gray) where $\overline{D}_{\text{Observed-SST}}$ is not significantly greater than $\overline{D}_{\text{Climatological-SST}}$ (MW test, $\alpha = 0.05$). (b) Variance ratio ($\sigma^2_{D,\text{Observed-SST}}/\sigma^2_{D,\text{Climatological}}$; dimensionless), masked where $\sigma^2_{D,\text{Observed-SST}}$ is not significantly greater than $\sigma^2_{D,\text{Climatological}}$ (RS test, $\alpha = 0.05$). (c) Maximum absolute difference d between cumulative distributions of drought duration (dimensionless), masked where differences are not statistically significant (KS test, $\alpha = 0.05$).

significant differences encompass 38.4% and 34.7% of the globe for droughts defined at the 24- and 48-month time scales, respectively (not shown). As discussed later, differences in dispersion are due to an increase in the occurrence of persistent droughts in the observed SST ensemble compared to the climatological SST ensemble.

Figure 6c shows the KS test statistic d for droughts defined at the 12-month time scale, calculated as the maximum absolute difference between empirical cumulative frequency distributions of drought durations in the observed and climatological SST ensembles, respectively (e.g., von Storch and Zwiers 1999); values are masked where there is no significant difference ($\alpha = 0.05$). Similar to the MW test, significant differences occur primarily over the tropics. Significant differences are, again, more widespread for droughts defined at the 3-month time scale, encompassing 72.7% of the globe; at the 24- and 48-month time scales, significant differences encompass 21.1% and 17.1% of the globe, respectively (not shown).

Closer inspection of drought durations reveals that significant differences in drought duration over mid- and high-latitude land regions are driven predominately by a small increase in the occurrence of persistent drought events. For example, the frequency of drought durations greater than 12 months (based on the 12-month SPI) over these regions in the observed SST ensemble is between 9 and 14 events per century, and the frequency of drought durations greater than 24 months is between 3 and 6 events per century; in the climatological SST ensemble, the frequency of durations greater than 12 and 24 months is generally between 7 and 11 events per century and between 2 and 5 events per century, respectively. Thus while persistent drought events occur in the absence of SST forcing, SST anomalies tend to increase their frequency throughout the tropics and some mid- and high-latitude regions.

c. Drought magnitude

Empirical distributions of drought magnitude were compared as for drought durations. As discussed in section 2, drought magnitude is defined as the mean monthly precipitation deficit during a drought event. For the MW and RS tests, we test the one-sided null hypotheses H_o: $\overline{M}_{\text{Observed-SST}} \leq \overline{M}_{\text{Climatological-SST}}$ and $\sigma^2_{M,\text{Observed-SST}} \leq \sigma^2_{M,\text{Climatological-SST}}$, where $\overline{M}_{\text{Observed-SST}}$ and $\overline{M}_{\text{Climatological-SST}}$ are the mean drought magnitudes for the observed and climatological SST ensembles, respectively, and $\sigma^2_{M,\text{Observed-SST}}$ and $\sigma^2_{M,\text{Climatological-SST}}$ are the interannual variances about their respective means.

Figure 7a shows the difference in mean drought magnitude between ensembles for droughts defined using the 12-month SPI, masked where $\overline{M}_{\text{Observed-SST}}$ is not significantly greater than $\overline{M}_{\text{Climatological-SST}}$. Significant differences occur throughout the tropics, with drought $\overline{M}_{\text{Observed-SST}}$ more than 25 mm month^{-1} greater than $\overline{M}_{\text{Observed-SST}}$ over the tropical Pacific. Regions of significant difference over midlatitudes are small and scattered, with differences in drought magnitude of 5–10 mm month^{-1}. SST anomalies contribute to a significant increase in drought magnitude over just 37.8% of the globe, including 35.0% of global land areas. Results

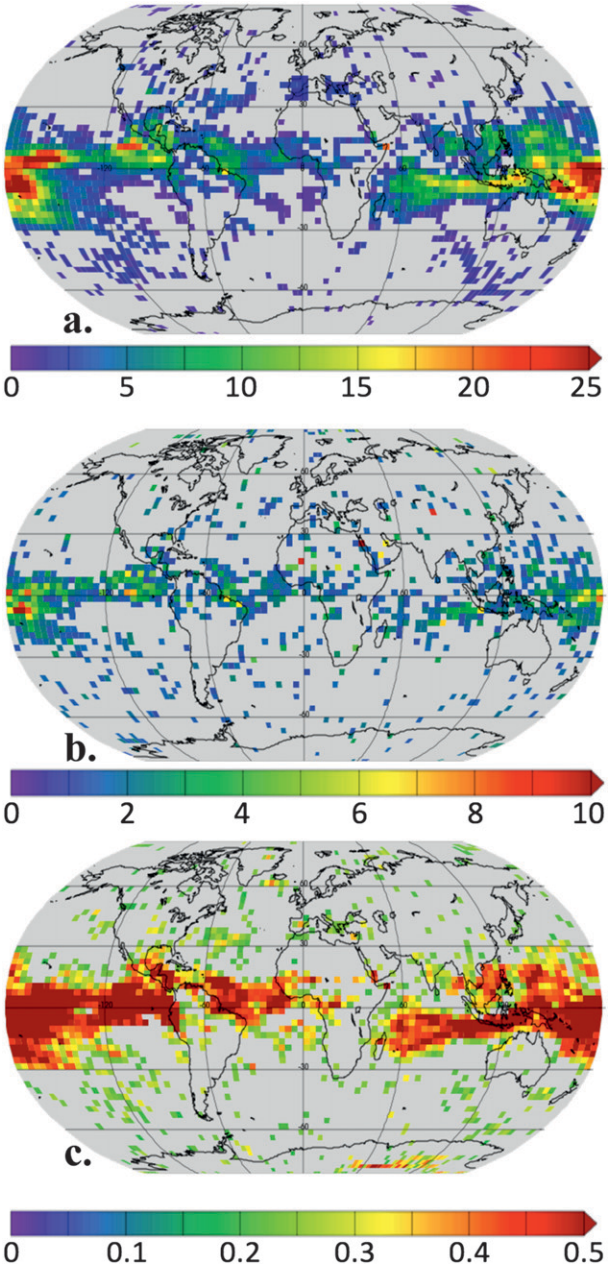

FIG. 7. As in Fig. 6, but for drought magnitudes.

are similar for the 3-, 24-, and 48-month time scales, with significant differences over 60.0%, 34.4%, and 30.0% of the globe, respectively (not shown).

Results of the RS test for drought magnitudes are shown in Fig. 7b. At the 12-month time scale, $\sigma^2_{M,\text{Observed}-\text{SST}}$ is more than twice $\sigma^2_{M,\text{Climatological}-\text{SST}}$ over the equatorial oceans. However, differences are statistically significant over just 21.2%, including 20.9% of global land areas. In particular, significant differences occur over few mid- and high-latitude land regions. Results are similar at other time scales, with 20.9%, 21.8%, and 19.9% of the globe exhibiting significant differences at the 3-, 24-, and 48-month time scales, respectively (not shown).

Results of the KS test for drought magnitudes are shown in Fig. 7c. Significant differences are again confined to the tropics and scattered grid cells over mid and high-latitudes, with 35.0% of the globe exhibiting significant differences ($\alpha = 0.05$). Results are similar for droughts at other time scales, though the spatial extent of significant differences is substantially greater at the 3-month time scale, with 73.4%, 31.6%, and 26.2% of the globe exhibiting significant differences at the 3-, 24-, and 48-month time scales, respectively (not shown).

At time scales of 12 months and longer, significant differences in drought durations and magnitudes between ensembles are largely confined to the tropics and midlatitude ocean regions, with few significant differences over midlatitude land regions. At the 3-month time scale, significant differences are much more widespread. Results suggest that SST anomalies have a strong influence on the duration and magnitude of short-term seasonal droughts. While SST anomalies contribute to a small increase in the occurrence of persistent drought events over some mid- and high-latitude land regions, they have no significant effect on drought characteristics over most regions outside of the tropics. However, the noisy spatial patterns of significant differences from all three tests are indicative of two inherent challenges in drought analysis—namely, droughts are by definition rare events and distributions of drought characteristics are noisy and strongly skewed. Even after compiling drought characteristics across ensemble members, detection of significant differences remains a challenge. Nonetheless, our results suggest that SST anomalies do not significantly contribute to the persistence or magnitude of multiyear drought events over most mid- and high-latitude regions.

5. Discussion

Here we use two ensembles of AGCM simulations forced with differing SST boundary conditions to investigate the influence of ocean–atmosphere forcing by SST anomalies on the long-term stochastic characteristics of precipitation and drought commonly used in water resources planning and management. Our results suggest that persistent SST anomalies significantly influence the long-term stochastic characteristics of precipitation throughout the tropics but over few midlatitude land regions. In the model used here, SST anomalies significantly influence seasonal mean precipitation over approximately 25% of the globe, suggesting that the precipitation response to SST anomalies is asymmetric over these regions (i.e., the precipitation response to positive SST forcing is roughly equal and opposite to the response to negative SST forcing). Differences in seasonal means occur mostly over transitions between characteristically wet and dry regions, including tropical–subtropical boundaries, and they suggest that a asymmetric response to SST anomalies results in a shift in large-scale features of the mean circulation. Consistent with previous studies (Koster et al. 2000), SST anomalies drive a significant increase in interannual variability of precipitation—and thus the magnitude of seasonal anomalies—over approximately 50% of the globe in the simulations evaluated here, including most of the tropics as well as some midlatitude regions.

Ocean–atmosphere forcing is shown to be the primary driver of season-to-season persistence of simulated precipitation anomalies throughout the tropics. SST anomalies have a weak influence on persistence over mid- and high latitudes; persistence is generally greater in simulations forced with observed SST compared to those with climatological SST, but the increase is statistically significant over few regions. The weak influence of SST anomalies on seasonal persistence over mid- and high latitudes stems from the chaotic nature of the atmosphere and stochastic nature of the midlatitude response to SST anomalies. Seasonal precipitation anomalies can be thought of as the sum of a SST-forced signal component, a land–atmosphere feedback component, and a (predominately high frequency) chaotic noise component (e.g., Rowell 1998; Koster et al. 2000; Zwiers et al. 2000). Outside of the tropics, precipitation variability is dominated by its noise component, with a significant influence of land–atmosphere feedbacks over some continental regions; precipitation response to SST anomalies, while statistically significant over many regions, is relatively small (e.g., Zwiers et al. 2000; Wu and Kirtman 2006). Thus while SST anomalies may persist from seasons to years, the persistent SST-forced signal is overshadowed by the large high-frequency noise component of seasonal precipitation over these regions and thus has no significant impact on season-to-season persistence of precipitation anomalies.

The weak influence of SST anomalies on the mean, amplitude, and persistence of simulated seasonal precipitation anomalies over mid- and high latitudes results in no significant change in the empirical distributions of drought frequency, duration, and magnitude between ensembles over these regions. As discussed earlier, numerous studies have shown significant relationships between SST anomalies and hydroclimatic variability on seasonal-to-decadal time scales. Similarly, a number of recent studies have shown a strong association between persistent SST anomalies and periods of widespread, persistent, and severe drought conditions (Hoerling and Kumar 2003; Schubert et al. 2004b; Seager et al. 2005; Seager 2007). These studies suggest that persistent SST anomalies are a significant driver of low-frequency hydroclimatic variability, including drought. By contrast, our results suggest that the large noise variance of seasonal precipitation anomalies and stochastic influence of SST anomalies on large-scale atmospheric circulation limit the influence of SST anomalies on extratropical precipitation and drought characteristics to seasonal time scales. For interannual and longer time scales, our results thus support recent conclusions that SST anomalies influence the timing of drought onset, while the magnitude and persistence of drought is predominately governed by other mechanisms—namely, land–atmosphere feedbacks (Hong and Kalnay 2000; Schubert et al. 2004a, 2008; Seager et al. 2008).

Importantly, our results demonstrate that in the AGCM used here, severe and sustained drought events may occur in the absence of anomalous SST forcing. While the frequency of multiyear droughts is slightly greater in the observed SST ensemble compared to the climatological SST ensemble, the occurrence of several severe and sustained droughts per century in the climatological SST ensemble suggests that these extreme events may arise due to chaotic atmospheric dynamics and land–atmosphere feedbacks alone. As shown in previous studies (Schubert et al. 2004a,b), the timing of drought events is strongly correlated between different simulations from the observed SST ensemble; however, it should be noted that the duration and magnitude of individual events varies widely between simulations—that is, the duration and magnitude of drought events are not reproducible based on SST boundary forcing. Results, again, support recent conclusions that the primary influence of SST anomalies is on the likelihood of drought during a given season and therefore on the timing of drought onset.

As noted in section 1, climate change is significantly altering the hydrologic cycle at global and regional scales. Results presented in this study are based on simulations of twentieth-century climate. Under future climate conditions, the physical mechanisms of hydroclimatic variability—including the relative contributions of ocean–atmosphere forcing and land–atmosphere feedbacks to the magnitude and persistence of drought events—may change because of changes in atmospheric heat and water vapor content (Santer et al. 2007), Hadley circulations (Seager et al. 2007; Seidel and Randel 2007), and the surface energy balance. Ocean heat uptake may significantly affect mean SST and their interannual variability, with subsequent effects on large-scale circulation and precipitation characteristics. In addition, the magnitude of land–atmosphere feedbacks is likely to increase during summer, which is associated with temperature-driven drying of soils and a stronger influence of soil moisture on the surface energy balance under increasingly moisture-limited conditions; however, increased drying may reduce the persistence of soil moisture anomalies and thus the time scale of land–atmosphere feedbacks. Further research is needed to evaluate the influence of SST anomalies on hydroclimatic variability under changing climate conditions.

Lastly, it should be noted that the results presented here are based on idealized numerical experiments and therefore cannot be directly confirmed by observations—indeed, the ability to perform such idealized experiments is a valuable property of models. As discussed in section 2, the NSIPP-1 AGCM was developed with particular emphasis on tropical ocean–atmosphere interaction, midlatitude stationary waves, and extratropical response to tropical SST anomalies (Bacmeister et al. 2000), and the observed SST simulations analyzed here largely reproduce salient features of observed seasonal precipitation anomalies. However, previous studies have shown that the midlatitude response to SST boundary forcing varies substantially among models, particularly at the regional scale (Shukla et al. 2000). Comparison of land–atmosphere coupling strength between models has also shown large differences over midlatitude continental regions, including particularly strong land–atmosphere feedbacks in the NSIPP-1 AGCM (Koster et al. 2004). Excessive land–atmosphere coupling in NSIPP-1 may mask the influence of SST anomalies on midlatitude drought characteristics. Similar studies with other models are needed to evaluate the potential model dependence of our results.

6. Conclusions

In the context of drought management, three questions are critical: When will the next drought begin? How long will it persist? And how severe will it be? Hydrologists and water resources managers have traditionally treated seasonal-to-interannual hydroclimatic

variability as purely random, and stochastic characterization of precipitation and drought is a critical component of water resources planning and management. For example, the design and operation of water resources systems and the allocation of water supplies is largely based on empirical distributions of precipitation and drought characteristics (e.g., Sadeghipour and Dracup 1985; Frick et al. 1990; Wilhite and Buchanan-Smith 2005; Steinemann and Cavalcanti 2006). However, recent studies demonstrating significant relationships between SST anomalies and drought occurrence have spurred much interest among both the forecasting and operations communities in the application of seasonal climate forecasts to drought planning and management, including the development and application of multiyear drought outlooks (e.g., Schubert et al. 2007).

Ocean–atmosphere forcing by persistent SST anomalies is the primary physical basis for today's state-of-the-art seasonal climate forecasts and long-range drought outlooks (e.g., Saha et al. 2006; Quan et al. 2006; Schubert et al. 2007; Livezey and Timofeyeva 2008). Numerous studies have shown that SST-based forecast systems are capable of predicting SST-forced changes in the probability distribution of seasonal precipitation during a given season—and therefore the likelihood of drought onset—over a number of midlatitude land regions. Our results suggest, however, that prospects for long-range SST-based forecasts of drought duration and magnitude are limited. While SST-based forecasts have the potential to significantly benefit short-term (1–3 month) water supply operations, long-term drought planning and management should be founded on robust characterization of the stochastic behavior of precipitation and drought.

Lastly, our results highlight an important difference between the climate science and water resources approaches to characterizing climate variability and drought. Water managers often rely on drought indices and ''triggers'' to implement drought management strategies (e.g., Wilhite and Buchanan-Smith 2005; Steinemann and Cavalcanti 2006; M. Roos 2006, personal communication). This threshold-based framework provides a practical and objective means of characterizing the stochastic nature of drought events; however, it does not account for the stochastic nature of the underlying processes. Notably, the threshold-based approach is not amenable to probabilistic seasonal forecast information. In addition to improving the skill and reliability of long-lead seasonal forecasts, forecasters and decision makers must work together to develop a common framework to integrate seasonal climate forecasts into drought planning and management.

REFERENCES

Adler, R. F., and Coauthors, 2003: The Version-2 Global Precipitation Climatology Project (GPCP) monthly precipitation analysis (1979–present). *J. Hydrometeor.,* **4,** 1147–1167.

Andreadis, K. M., E. A. Clark, A. W. Wood, A. F. Hamlet, and D. P. Lettenmaier, 2005: Twentieth-century drought in the conterminous United States. *J. Hydrometeor.,* **6,** 985–1001.

Arakawa, A., and W. H. Schubert, 1974: Interaction of a cumulus cloud ensemble with large-scale environment. *J. Atmos. Sci.,* **31,** 674–701.

Bacmeister, J. T., P. J. Pegion, S. D. Schubert, and M. J. Suarez, 2000: Atlas of seasonal means simulated by the NSIPP-1 atmospheric GCM. NASA Tech. Memo. NASA/TM-2000-104606/VOL17, 218 pp.

Barnett, T. P., and Coauthors, 2008: Human-induced changes in the hydrology of the western United States. *Science,* **319,** 1080–1083.

Bates, B. C., Z. W. Kundzewicz, S. Wu, and J. P. Palutikof, Eds., 2008: Climate Change and water. Intergovernmental Panel on Climate Change Tech. Paper VI, 214 pp.

California DWR, 2000: Preparing for California's next drought: Changes since 1987-1992. 66 pp.

Dracup, J. A., and E. Kahya, 1994: The relationships between United States streamflow and La Nina events. *Water Resour. Res.,* **30,** 2133–2141.

Eltahir, E. A. B., 1998: A soil moisture–rainfall feedback mechanism 1. Theory and observations. *Water Resour. Res.,* **34,** 765–776.

Findell, K. L., and E. A. B. Eltahir, 1997: An analysis of the soil moisture-rainfall feedback, based on direct observations from Illinois. *Water Resour. Res.,* **33,** 725–735.

Fischer, E. M., S. I. Seneviratne, D. Lüthi, and C. Schär, 2007: Contribution of land-atmosphere coupling to recent European summer heat waves. *Geophys. Res. Lett.,* **34,** L06707, doi:10.1029/2006GL029068.

Folland, C., J. Shukla, J. Kinter, and M. Rodwell, 2002: The climate of the twentieth century project. *CLIVAR Exchanges,* No. 7, International CLIVAR Project Office, Southampton, United Kingdom, 37–39.

Frick, D. M., D. Bode, and J. D. Salas, 1990: Effect of drought on urban water supplies 1: Drought analysis. *J. Hydraul. Eng.,* **116,** 733–753.

Graham, N. E., and T. P. Barnett, 1987: Sea-surface temperature, surface wind divergence, and convection over the tropical oceans. *Science,* **238,** 657–659.

Guttman, N. B., 1999: Accepting the standardized precipitation index: A calculation algorithm. *J. Amer. Water Resour. Assoc.,* **35,** 311–322.

Hayes, M. J., M. D. Svoboda, D. A. Wilhite, and O. V. Vanyarkho, 1999: Monitoring the 1996 drought using the standardized precipitation index. *Bull. Amer. Meteor. Soc.,* **80,** 429–438.

Hidalgo, H. G., 2004: Climate precursors of multidecadal drought variability in the western United States. *Water Resour. Res.,* **40,** W12504, doi:10.1029/2004WR003350.

Hoerling, M. P., and A. Kumar, 2003: The perfect ocean for drought. *Science,* **299,** 691–694.

Hong, S. Y., and E. Kalnay, 2000: Role of sea surface temperature and soil moisture feedback in the 1998 Oklahoma-Texas drought. *Nature,* **408,** 842–844.

Ji, L., and A. J. Peters, 2003: Assessing vegetation response to drought in the northern Great Plains using vegetation and drought indices. *Remote Sens. Environ.,* **87,** 85–98.

Keyantash, J., and J. A. Dracup, 2002: The quantification of drought: An evaluation of drought indices. *Bull. Amer. Meteor. Soc.,* **83,** 1167–1180.

Koster, R. D., and M. J. Suarez, 1996: The influence of land surface moisture retention on precipitation statistics. *J. Climate,* **9,** 2551–2567.

——, ——, and M. Heiser, 2000: Variance and predictability of precipitation at seasonal-to-interannual timescales. *J. Hydrometeor.,* **1,** 26–46.

——, ——, R. W. Higgins, and H. M. Van den Dool, 2003: Observational evidence that soil moisture variations affect precipitation. *Geophys. Res. Lett.,* **30,** 1241, doi:10.1029/2002GL016571.

——, and Coauthors, 2004: Regions of strong coupling between soil moisture and precipitation. *Science,* **305,** 1138–1140.

Livezey, R. E., and W. Y. Chen, 1983: Statistical field significance and its determination by Monte Carlo techniques. *Mon. Wea. Rev.,* **111,** 46–59.

——, and M. M. Timofeyeva, 2008: The first decade of long-lead U.S. seasonal forecasts. *Bull. Amer. Meteor. Soc.,* **89,** 843–854.

Lloyd-Hughes, B., and M. A. Saunders, 2002: A drought climatology for Europe. *Int. J. Climatol.,* **22,** 1–14.

Lorenz, E. N., 1963: Deterministic nonperiodic flow. *J. Atmos. Sci.,* **20,** 130–141.

Maidment, D. R., Ed., 1993: *Handbook of Hydrology*. McGraw-Hill, 1424 pp.

McCabe, G. J., M. A. Palecki, and J. L. Betancourt, 2004: Pacific and Atlantic Ocean influences on multidecadal drought frequency in the United States. *Proc. Natl. Acad. Sci. USA,* **101,** 4136–4141.

McKee, T. B., N. J. Doesken, and J. Kleist, 1993: The relationship of drought frequency and duration to timescales. Preprints, *Eighth Conf. on Applied Climatology,* Anaheim, CA, Amer. Meteor. Soc., 179–184.

Mishra, A. K., and V. Desai, 2005: Drought forecasting using stochastic models. *Stochastic Environ. Res. Risk Assess.,* **19,** 326–399.

Moorthi, S., and M. J. Suarez, 1992: Relaxed Arakawa–Schubert: A parameterization of moist convection for general circulation models. *Mon. Wea. Rev.,* **120,** 978–1002.

Nalbantis, I., and G. Tsakiris, 2009: Assessment of hydrological drought revisited. *Water Resour. Manage.,* **23,** 881–897.

NOAA, cited 2009: Climate of 2009—January U.S. standardized precipitation index. [Available online at http://lwf.ncdc.noaa.gov/oa/climate/research/prelim/drought/spi.html.]

Palmer, T. N., 2000: Predicting uncertainty in forecasts of weather and climate. *Rep. Prog. Phys.,* **63,** 71–116.

Pegion, P. J., and A. Kumar, 2008: Analysis of the multi-model US CLIVAR drought working group simulations. *CLIVAR Exchanges,* No. 6, International CLIVAR Project Office, Southampton, United Kingdom, 6–8.

Quan, X., M. Hoerling, J. Whitaker, G. Bates, and T. Xu, 2006: Diagnosing sources of U.S. seasonal forecast skill. *J. Climate,* **19,** 3279–3293.

Quiring, S. M., and G. B. Goodrich, 2008: Nature and causes of the 2002 to 2004 drought in the southwestern United States compared with the historic 1953 to 1957 drought. *Climate Res.,* **36,** 41–52.

Rayner, N. A., D. E. Parker, E. B. Horton, C. K. Folland, L. V. Alexander, D. P. Rowell, E. C. Kent, and A. Kaplan, 2003: Global analyses of sea surface temperature, sea ice, and night marine air temperature since the late nineteenth century. *J. Geophys. Res.,* **108,** 4407, doi:10.1029/2002JD002670.

Redmond, K. T., and R. W. Koch, 1991: Surface climate and streamflow variability in the western United States and their relationship to large-scale circulation indices. *Water Resour. Res.,* **27,** 2381–2399.

Ropeleski, C. F., and M. S. Halpert, 1987: Global and regional scale precipitation patterns associated with the El Niño/Southern Oscillation. *Mon. Wea. Rev.,* **115,** 1606–1626.

Rowell, D. P., 1998: Assessing potential seasonal predictability with an ensemble of multidecadal GCM simulations. *J. Climate,* **11,** 109–120.

Sadeghipour, J., and J. A. Dracup, 1985: Regional frequency analysis of hydrologic multiyear droughts. *Water Resour. Bull.,* **21,** 481–487.

Saha, S., and Coauthors, 2006: The NCEP climate forecast system. *J. Climate,* **19,** 3483–3517.

Santer, B. D., and Coauthors, 2007: Identification of human-induced changes in atmospheric moisture content. *Proc. Natl. Acad. Sci. USA,* **104,** 15 248–15 253.

Schubert, S. D., M. J. Suarez, P. J. Pegion, R. D. Koster, and J. D. Bacmeister, 2004a: Causes of long-term drought in the U.S. Great Plains. *J. Climate,* **17,** 485–503.

——, ——, ——, ——, and ——, 2004b: On the cause of the 1930s Dust Bowl. *Science,* **303,** 1855–1859.

——, R. D. Koster, M. P. Hoerling, R. Seager, D. Lettenmaier, A. Kumar, and D. Gutzler, 2007: Predicting drought on seasonal-to-decadal timescales. *Bull. Amer. Meteor. Soc.,* **88,** 1625–1630.

——, M. J. Suarez, P. J. Pegion, R. D. Koster, and J. T. Bacmeister, 2008: Potential predictability of long-term drought and pluvial conditions in the U.S. Great Plains. *J. Climate,* **21,** 802–816.

Seager, R., 2007: The turn of the century North American drought: Global context, dynamics, and past analogs. *J. Climate,* **20,** 5527–5552.

——, Y. Kushnir, C. Herweijer, N. Naik, and J. Velez, 2005: Modeling of tropical forcing of persistent droughts and pluvials over western North America: 1856–2000. *J. Climate,* **18,** 4065–4088.

——, and Coauthors, 2007: Model Projections of an Imminent Transition to a More Arid Climate in Southwestern North America. *Science,* **316,** 1181–1184.

——, Y. Kushnir, M. Ting, M. Cane, N. Naik, and J. Miller, 2008: Would advanced knowledge of the 1930s SSTs have allowed prediction of the Dust Bowl drought? *J. Climate,* **21,** 3261–3281.

Seidel, D. J., and W. J. Randel, 2007: Recent widening of the tropical belt: Evidence from tropopause observations. *J. Geophys. Res.,* **112,** D20113, doi:10.1029/2007JD008861.

Seiler, R. A., M. J. Hayes, and L. Bressan, 2002: Using the standardized precipitation index for flood risk monitoring. *Int. J. Climatol.,* **22,** 1365–1376.

Sheffield, J., G. Goteti, F. Wen, and E. F. Wood, 2004: A simulated soil moisture based drought analysis for the United States. *J. Geophys. Res.,* **109,** D24108, doi:10.1029/2004JD005182.

Shukla, J., and Coauthors, 2000: Dynamical seasonal prediction. *Bull. Amer. Meteor. Soc.,* **81,** 2593–2606.

Sims, A. P., D. D. S. Niyogi, and S. Raman, 2002: Adopting drought indices for estimating soil moisture: A North Carolina case study. *Geophys. Res. Lett.,* **29,** 1183, doi:10.1029/2001GL013343.

Steinemann, A., and L. F. N. Cavalcanti, 2006: Developing multiple indicators and triggers for drought plans. *J. Water Resour. Plann. Manage.,* **132,** 164–174.

Straus, D., J. Shukla, D. Paulino, S. D. Schubert, M. J. Suarez, P. J. Pegion, and A. Kumar, 2003: Predictability of the seasonal

mean atmospheric circulation during autumn, winter, and spring. *J. Climate,* **16,** 3629–3649.

Suarez, M. J., and L. L. Takacs, 1995: Documentation of the AIRES/GEOS Dynamical Core Version 2. NASA Tech. Memo. NASA-TM-104606-VOL-5, 56 pp.

Van den Dool, H. M., and R. M. Chervin, 1986: A comparison of month-to-month persistence of anomalies in a general circulation model and in the earth's atmosphere. *J. Atmos. Sci.,* **43,** 1454–1466.

von Storch, H., and F. W. Zwiers, 1999: *Statistical Analysis in Climate Research*. Cambridge University Press, 484 pp.

Wilhite, D. E., and M. Buchanan-Smith, 2005: Drought as hazard: Understanding the natural and social context. *Drought and Water Crises: Science, Technology, and Management Issues,* Taylor and Francis, 3–32.

WRCC, cited 2009: One-month standardized precipitation index through the end of January 2009. [Available online at http://www.wrcc.dri.edu/cgi-bin/spiFmap.pl?spi01.]

Wu, R. G., and B. P. Kirtman, 2006: Changes in spread and predictability associated with ENSO in an ensemble of coupled GCM simulations. *J. Climate,* **19,** 4378–4396.

Zar, J. H., 1999: *Biostatistical Analysis*. 4th ed. Prentice Hall, 929 pp.

Zwiers, F. W., X. L. Wang, and J. Sheng, 2000: Effects of specifying bottom boundary conditions in an ensemble of atmospheric GCM simulations. *J. Geophys. Res.,* **105,** 7295–7315.